

Article

Modeling of Fuzzy Cognitive Maps with a Metaheuristics-Based Rainfall Prediction System

Mesfer Al Duhayyim ^{1,*}, Heba G. Mohamed ², Jaber S. Alzahrani ³, Rana Alabdan ⁴, Mohamed Mousa ⁵, Abu Sarwar Zamani ⁶, Ishfaq Yaseen ⁶ and Mohamed Ibrahim Alsaid ⁶

- ¹ Department of Computer Science, College of Computer Engineering and Sciences, Prince Sattam bin Abdulaziz University, Al-Kharj 16273, Saudi Arabia
- ² Department of Electrical Engineering, College of Engineering, Princess Nourah bint Abdulrahman University, Riyadh 11671, Saudi Arabia
- ³ Department of Industrial Engineering, College of Engineering at Alqunfudah, Umm Al-Qura University, Mecca 24382, Saudi Arabia
- ⁴ Department of Information Systems, College of Computer and Information Science, Majmaah University, Al-Majmaah 11952, Saudi Arabia
- ⁵ Department of Electrical Engineering, Faculty of Engineering and Technology, Future University in Egypt, New Cairo 11845, Egypt
- ⁶ Department of Computer and Self Development, Preparatory Year Deanship, Prince Sattam bin Abdulaziz University, Al-Kharj 16278, Saudi Arabia
- * Correspondence: m.alduhayyim@psau.edu.sa

Abstract: Rainfall prediction remains a hot research topic in smart city environments. Precise rainfall prediction in smart cities becomes essential for planning security measures before construction and transportation activities, flight operations, water reservoir systems, and agricultural tasks. Precise rainfall forecasting now becomes more complex than before because of extreme climatic changes. Machine learning (ML) approaches can forecast rainfall by deriving hidden patterns from historic meteorological datasets. Selecting a suitable classification method for forecasting has become a tough job. This article introduces the Fuzzy Cognitive Maps with a Metaheuristics-based Rainfall Prediction System (FCMM-RPS) technique. The intention of the FCMM-RPS technique is to predict rainfall automatically and efficiently. To accomplish this, the presented FCMM-RPS technique primarily pre-processes the rainfall data to make it compatible. In addition, the presented FCMM-RPS technique predicts rainfall using the FCM model. To enhance the rainfall prediction outcomes of the FCM model, the parameter optimization process is performed using a modified butterfly optimization algorithm (MBOA). The performance assessment of the FCMM-RPS technique is tested on a rainfall dataset. A widespread comparison study highlights the improvements of the FCMM-RPS technique in the rainfall forecasting process compared to existing techniques with a maximum accuracy of 94.22%.

Keywords: rainfall forecasting; weather; machine learning; artificial intelligence; parameter optimization



Citation: Al Duhayyim, M.; Mohamed, H.G.; Alzahrani, J.S.; Alabdan, R.; Mousa, M.; Zamani, A.S.; Yaseen, I.; Alsaid, M.I. Modeling of Fuzzy Cognitive Maps with a Metaheuristics-Based Rainfall Prediction System. *Sustainability* **2023**, *15*, 25. <https://doi.org/10.3390/su15010025>

Academic Editors: Daniel Stys, Sabina Kordana-Obuch, Kamil Pochwat and Mariusz Starzec

Received: 16 October 2022
Revised: 14 December 2022
Accepted: 15 December 2022
Published: 20 December 2022



Copyright: © 2022 by the authors. Licensee MDPI, Basel, Switzerland. This article is an open access article distributed under the terms and conditions of the Creative Commons Attribution (CC BY) license (<https://creativecommons.org/licenses/by/4.0/>).

1. Introduction

Rainfall is the most significant phenomenon within a climate system and its chaotic nature has a direct effect on biological systems, water resource planning, and agriculture [1]. In finance, the rainfall level for a specific period is essential to predict the value of financial security. Currently, the abilities of scientists in predicting and understanding rainfall have been augmented because of several methods formulated to raise the precision level in rainfall prediction [2]. Rainfall forecasting is useful to prevent floods, which saves the properties and lives of humans. Additionally, it aids in managing water resources. Data for information relating to rainfall in advance assists agriculturalists in managing their crops better [3]. Variation in rainfall quantity and timing makes rainfall prediction a difficult task for weather-related scientists [4]. Rainfall derivatives share the same principles with other regular and climate variations. It is the agreement between two or more, in which the

contract value relies on the basic financial asset. Therefore, in the case of rainfall prediction, the basic asset will be a climate type, like rainfall [5]. One important variance among weather and common derivatives is that the primary asset that decides the price of the contract is not tradable. Consequently, several existing techniques in the literature for other derivatives are inappropriate for predicting rainfall prediction [6].

The conventional techniques use statistical approaches to measure the correlations among rainfall, geographic coordinates (like longitude and latitude), and other elements (like wind speed, pressure, humidity, and temperature) [7]. However, the complexity of these elements and rainfall's non-linearity make it tough to forecast. Accordingly, efforts have been made to diminish this nonlinearity by utilizing Wavelet analysis, Singular Spectrum Analysis, and Empirical Mode Decompositions, among others [8]. However, the statistical and mathematical approaches used required more time and complicated computation with minimal effects. The estimation of rainfall derivatives imposes various hindrances, both in finance and research [9]. A light amount of the literature has investigated rainfall derivatives, since the concept is new, along with the fact that rainfall is hard to measure precisely. In financial practice, investors even share similar forms of problems, deterring the trading of weather derivatives in monetary markets [10]. Thus, the aim was to formulate a technique for precise weather forecasting, which must reduce the practical risk from investors. Accurate rainfall forecasting is a challenging process because of extreme climate variations. Artificial intelligence (AI) approaches can forecast rainfall via the extraction of hidden patterns from past weather data.

Accurate rainfall prediction becomes challenging because of extreme climate variations. Particularly, precise and timely rainfall prediction can be useful for planning and security measures for flight operation, agriculture, water reservoir management, construction, and transportation activities. A red alert in advance in the case of extreme rainfall can save the citizens of smart cities from potentially life-threatening situations. AI techniques can predict rainfall by extracting hidden patterns from historical weather data. Moreover, the selection of proper classification techniques for prediction is a difficult job.

To resolve these issues, this article introduces the Fuzzy Cognitive Maps with a Metaheuristics-based Rainfall Prediction System (FCMM-RPS) technique. The intention of the FCMM-RPS technique is to predict rainfall automatically and efficiently. To accomplish this, the presented FCMM-RPS technique primarily preprocesses the rainfall data to make it compatible. In addition, the presented FCMM-RPS technique predicts rainfall using the FCM model. To enhance the rainfall prediction outcomes of the FCM model, the parameter optimization process is performed using a modified butterfly optimization algorithm (MBOA). The MBOA is chosen due to its simplicity, easy implementation, and high stability. The performance assessment of the FCMM-RPS technique is tested on a rainfall dataset.

The rest of the paper is organized as follows. Existing rainfall prediction models are discussed in Section 2, and Section 3 introduces the proposed FCMM-RPS technique. Next, Section 4 offers performance validation and Section 5 draws conclusions.

2. Related Works

Rahman et al. [11] devise a new real-time rainfall prediction system for smart cities utilizing a machine learning (ML) fusion method. This modeled structure employs four commonly employed supervised ML approaches. For effective rainfall forecasting, the fuzzy logic (FL) method was used in the structure for integrating the prediction accuracy of the ML approach called fusion. Pathan et al. [12] proposed an effective approach for predicting rainfall events for dimensionality reductions. Initially, the authors detected appropriate features from weather data that had a main contribution to rainfall forecasting utilizing a wrapper-oriented feature selection (FS) approach. Then, principal component analysis (PCA) was compiled with the complete data along with the selected feature data to minimize the data dimensionality. Poornima and Pushpalatha [13] offered an intensified long short-term memory (LSTM)-oriented recurrent neural network (RNN) for rainfall

forecasting. The neural network (NN) was tested and trained with a standard rainfall dataset. The well-trained network produced estimated features of rainfall.

He et al. [14] modeled a hybrid method STL-ML (seasonal trend decomposition and ML) to forecast the rainfall time series in advance related to historic rainfall and other atmospheric data. This STL-ML method has three steps: firstly, the forecasted rainfall is acquired through the inclusion of the predicted values of the three elements, and many metrics are employed for assessing the performance of the method. Secondly, the seasonal trend decomposition is leveraged for decomposing the rainfall time series into the remainder, trend, and seasonal elements. Lastly, three different ML methods such as the LightGBM model, GRU network, and multi-time scale are formulated to forecast the three elements. In [15], artificial neural networks (ANNs) such as the Feed Forward NN (FFNN) method were framed to forecast rainfall. ANNs are considered an attractive and valuable soft-computing technique for forecasting. ANN depends on a self-adaptive system where the method learns from historic data capturing functional relationships among data and making forecasts on present data.

Wei and Chou [16] devised a Hadoop Spark distribution structure related to big-data technology for hastening the computation of typhoon rainfall forecasting approaches. This work leveraged multiple linear regression (MLR) and deep neural networks (DNNs) in ML, for enforcing rainfall forecasting approaches and assessing the accuracy level of rainfall forecasting. The Hadoop Spark distributed cluster-computing structure is the big-data technology employed. Samad et al. [17] utilized an LSTM-related RNN for forecasting rainfall. Standard datasets were employed for the testing and training of the developed method. The time series rainfall datasets were pre-processed through Additive Seasonal Decomposition to enhance the prediction analysis. The preprocessed datasets were then put through the method. ANN was applied for benchmarking the LSTM method. In spite of the several models existing in earlier studies, there is still a need to enhance the weather forecasting performance. At the same time, most of the existing works do not focus on the parameter-tuning process. The parameters in the classification model mainly influence its overall performance in the rainfall prediction process. Since the trial and error method for parameter tuning is a tedious and erroneous process, metaheuristic algorithms can be applied. At the same time, the FCM parameters can affect the performance of the fuzzy system irrespective of the significance. Therefore, in this work, MBOA is applied for the parameter optimization of the FCM model.

3. The Proposed Model

In this article, we have introduced a new FCMM-RPS technique for predicting rainfall accurately. The major aim of the FCMM-RPS technique is to forecast rainfall routinely and efficiently. It follows a three-step process: data pre-processing, FCM-based prediction, and MBOA-based parameter tuning. Figure 1 depicts the workflow of the FCMM-RPS system.

3.1. Data Pre-Processing

The presented FCMM-RPS technique primarily pre-processes the rainfall data to make it compatible. Initially, the data cleaning process takes place where the missing values in the dataset are replaced by the mean method. Then, normalization is applied to convert the data into a scalar format. In this work, min–max normalization [18] is used to normalize the input data into the range of 0 to 1. By assuming feature X , such that it contains a mapping from the dataset among X_{\min} and X_{\max} , min–max normalization (X_{norm}) is attained by the following:

$$X_{norm} = \frac{X - X_{\min}}{X_{\max} - X_{\min}}, \quad (1)$$

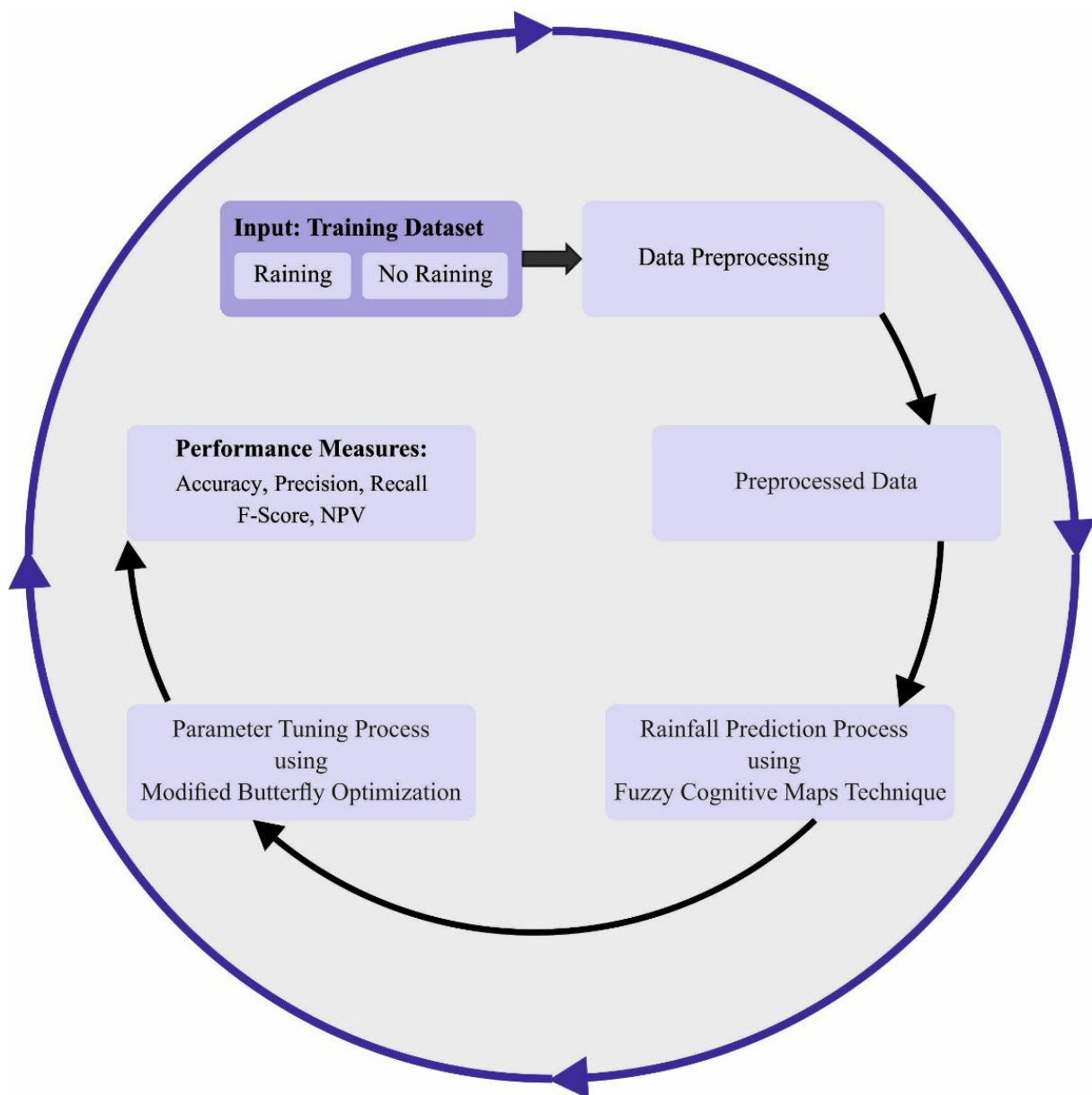


Figure 1. Workflow of FCMM-RPS system.

3.2. Rainfall Prediction using FCM Model

In this study, the presented FCMM-RPS technique predicts rainfall using the FCM model. In the classification method, the weather data is passed into the FCM model for the prediction process. FCM is regarded as an RNN, utilizing interpretability features that are widely applied in modeling tasks [19]. They encompass a group of neural processing entities called concept (neuron) and causal relationships. The activation value of these neurons usually takes values in the range of zero and one; thus, the stronger the activation value, the greater its effects on the model. Connected weight is pertinent in these systems. The power of the causal relationships between concepts C_i and C_j are measured by $w_{ij} \in [-1, 1]$ arithmetical weight and signified by a causal edge from C_i to C_j . There exist three possible types of causal relationships amongst neural processing units in FCM-based networks that state the impacts from a single neuron to others, as shown below:

- If $w_{ij} > 0$, a rise (decrement) in the cause C_i produces an increment (decrement) in impact C_j with intensity $|w_{ij}|$.

- If $w_{ij} < 0$, a rise (decrement) in the cause C_i produces a decrement (increment) in neuron C_j with intensity $|w_{ij}|$.
- If $w_{ij} = 0$, there exists no causal relationships between C_i and C_j . These rules are reiterated until a stopping condition is fulfilled. A new activation vector can be evaluated at each step t and then a predetermined number of iterations [20]. The FCM is stated to have converged if it obtains a fixed-point attractor, otherwise, the update process ends after a maximum number of iterations T is accomplished.

$$A_i^{(t+1)} = f\left(\sum_{j=1}^M w_{ji} A_j^{(t)}\right), i \neq j, \quad (2)$$

where $f(\cdot)$ signifies monotonically non-reducing nonlinear functions exploited for clamping the activation value of each neuron to the interval. For example, the trivalent function, sigmoid variants, and bivalent function. Next, emphasize the sigmoid function since it has demonstrated better prediction capabilities. In the study, a non-linear transfer function is used where λ signifies the sigmoid slope and h denotes the offset. Several research workers have discovered that these parameters are closely connected with network convergence.

$$f(A_i) = \frac{1}{1 + e^{-\lambda(A_i - h)}}, \quad (3)$$

These rules are chosen while upgrading the activation values of neuron that is not influenced by the neural processing entities.

$$A_i^{(t+1)} = f\left(\sum_{j=1}^M w_{ji} A_j^{(t)} + A_i^{(t)}\right), i \neq j, \quad (4)$$

An alternate adapted upgrading rule was introduced to avoid the conflicts that emerged in the event of non-active neurons. The rescaled inference enables us to deal with the scenario where there exist no data regarding the initial state of the neuron and helps to avoid saturation problems.

$$A_i^{(t+1)} = f\left(\sum_{j=1}^M w_{ji} (2A_j^{(t)} - 1) + (2A_i^{(t)} - 1)\right), i \neq j, \quad (5)$$

The model generates a similar output once the cognitive network has the capacity to converge, and the activation number of neurons remains the same. Simultaneously, a cyclic FCM generates various responses, with the exception of some states that are usually produced. The last possible scenario is related to the chaotic configuration where the network generates dissimilar state vectors.

3.3. Parameter Tuning Using MBOA

To enhance the rainfall prediction outcomes of the FCM model, the parameter optimization process is performed using the MBOA. BOA is based on the food-foraging behaviors of butterflies and is applied as a searching agent to perform optimization in BOA [21]. Butterflies have a sense receptor that is applied for smelling or sensing the odor of food or flowers. These sense receptors are named chemoreceptors and are dispersed over the butterfly's body parts. The presented method assumes that the butterfly produces scent or fragrance with certain power or intensity. The fragrance that rises from the butterfly is sensed by the different butterflies present in the neighborhood and an aggregate social learning scheme is framed. This fragrance is related to the fitness of the butterfly, which is evaluated by the objective function. This represents that when the butterfly moves around in the searching region, the fitness could have similarly changed. When the butterfly is unable to detect the scent of others in the searching space, then it makes random strides and this is named a local searching technique. Then, when the butterfly senses fragrance

from the optimum butterfly in the search space, it moves toward the optimum butterflies, which is named a global searching technique and can be formulated as follows:

$$pf_i = cI^a, \quad (6)$$

In Equation (6), c represents the sensory modality, a characterizes the power exponent based on modality that is accountable for distinct levels of absorption, pf_i , characterize the perceived magnitude of scent viz., how strongly the fragrance of i^{th} butterflies are perceived by other butterflies present in the region, and I shows the stimulus intensity. Figure 2 demonstrates the steps involved in BOA.

$$x_{i^{t+1}} = x_i^t + F_i^{t+1}, \quad (7)$$

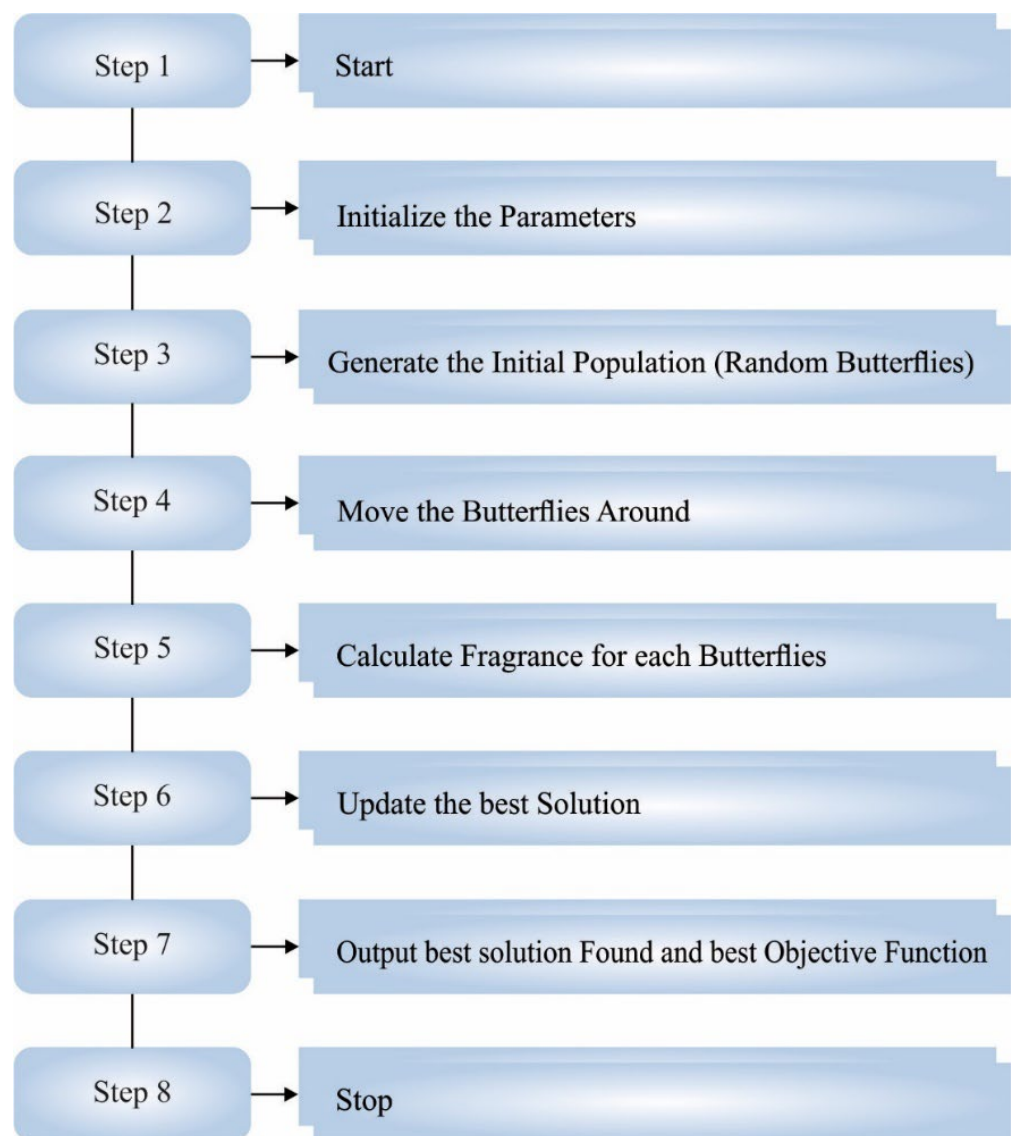


Figure 2. Steps involved in BOA.

Now, F_i represents the fragrance that is used by x_i^{th} butterflies to upgrade the position during iteration and x_i^t signifies the solution vector x_i for i^{th} butterflies at t iteration count. Furthermore, there exist two major stages, global and local search stages. During the global search technique, the butterfly takes a step toward the appropriate solution or butterfly g^* in the following:

$$F_i^{t+1} = (r^2 \times g^* - x_i^t) \times pf_i, \quad (8)$$

In Equation (8), g^* represents the existing optimum solution amongst the existing iterations, pf_i denotes the perceived fragrance of i^{th} butterflies, and r shows the random number ranges from zero to one:

$$F_i^{t+1} = (r^2 \times x_{j^t} - x_{k^t}) \times pf_i, \quad (9)$$

In Equation (9), x_{j^t} and x_{k^t} characterize j^{th} and k^{th} butterflies from the solution space. If x_{j^t} and x_{k^t} belong to a similar population and r represents the random number ranges from zero to one. A switching possibility p is employed in BOA for switching from global searching to intensive local searching. The pseudocode of BOA is demonstrated in Algorithm 1.

Algorithm 1: Pseudocode for BOA

The main function $f(x)$, $x = (x_1, x_2, x_d)$
 Generate the population of n butterflies $x_i = (i = 1, 2, n)$
 Define the switch probabilities p , sensor modality c , and power exponents a
 while ending criteria are not satisfied do
 for every butterfly bf from the population do
 Calculate the fragrance to bf based on Equation (6)
 end for
 Determine the optimal bf
 for every butterfly bf from the population do
 Generate the arbitrary value rand within 0 and 1
 if $rand < p$ then
 Move near the optimal butterfly
 else
 Move arbitrarily based on Equations (7) and (9)
 end if
 Evaluate a novel butterfly
 If the novel butterfly is optimal, upgrade it from the population
 end for
 Upgrade the value of c
 Determine the existing global optimal butterfly
 end while
 Output the optimal solution.

In the MBOA, the BOA is integrated into the Levy Flight (LF) concept. The LF monitors the rule of the Levy distribution of several arbitrary phenomena like random walk, Brownian motion, and so on [22]. Presently, LF is frequently employed in intelligent optimization. For instance, the BOA implements LF for updating the place. LF develops the searching space, therefore it can be simpler to avoid premature convergence by introducing LF into the MBO approach.

LF place upgrades to:

$$x_i(t+1) = \begin{cases} x_j(t) + \alpha \oplus Levy(\lambda) & f(x_j(t)) \leq f(v_i(t+1)) \\ v_i(t+1) & f(x_j(t)) > f(v_i(t+1)) \end{cases}, \quad (10)$$

where x_i^t defines the t^{th} generation place of x_i , \oplus implies the dot multiplication, α denotes the step size control parameter, and Levy (λ) implies the arbitrary searching path that fulfills:

$$\text{Levy} \sim u = t^{-\lambda}, 1 < \lambda \leq 3, \quad (11)$$

The step size observes the Levy distribution, and step size s is computed as:

$$s = \frac{\mu}{|v|^{1/\beta}}, \quad (12)$$

In which μ , v are normally distributed, determined as:

$$\mu \sim N(0, \sigma_\mu^2), \quad (13)$$

$$v \sim N(0, \sigma_v^2), \quad (14)$$

whereas

$$\sigma_\mu = \frac{(1 + \beta) \left(\sin \frac{\pi\beta}{2} \right)}{\frac{1+\beta}{2} \beta^{\frac{\beta-1}{2}}}, \quad (15)$$

$$\sigma_v = 1, \quad (16)$$

In which β is generally a constant of 1.5.

The MBOA approach develops a fitness function (FF) for realizing superior classifier results. It defines a positive integer for exemplifying the good efficiency of candidate solutions. During this work, the minimized classifier error rate assumes that FF is expressed in Equation (17).

$$\text{fitness}(x_i) = \frac{\text{number of misclassified samples}}{\text{Total number of samples}} * 100, \quad (17)$$

4. Experimental Validation

The proposed model is simulated using Python tool. The rainfall prediction results of the FCMM-RPS model are tested using a dataset [11] comprising 25,919 samples under two classes, as defined in Table 1. The dataset consists of 25,919 instances and 11 features, out of which 10 features are independent and 1 is dependent (output class). The features are temperature ($^{\circ}\text{C}$), atmospheric pressure (weather station), atmospheric pressure (sea level), pressure tendency, relative humidity (%), mean wind speed, minimum temperature, maximum temperature, visibility (km), and dew point temperature ($^{\circ}\text{C}$). Further, the dataset is preprocessed to improve the quality of the rainfall data over two days. Initially, the missing values in the data are replaced by the mean method. Next, min–max normalization is used to scale the data into a uniform scale of [0, 1].

Table 1. Dataset details.

Class	No. of Samples
Positive (rainfall)	23,682
Negative (no rainfall)	2237
Total Number of Samples	25,919

The performance measures used to examine the rainfall prediction are defined as follows. Accuracy ($Accu_y$) represents the number of correctly classified instances to the total number of instances.

$$Accu_y = \frac{TP + TN}{TP + TN + FP + FN} \quad (18)$$

Precision ($Prec_n$) is defined as the ratio of properly classified positive samples to the total number of classified positive samples.

$$Prec_n = \frac{TP}{TP + FP} \quad (19)$$

The recall ($Reca_l$) is calculated as the ratio between the number of positive samples correctly classified as positive to the total number of positive samples.

$$Reca_l = \frac{TP}{TP + FN} \quad (20)$$

The F-score (F_{score}) is the harmonic mean of a system's precision and recall values. It can be calculated by the following formula:

$$F_{score} = 2 * \left(\frac{Prec_n * Reca_l}{Prec_n + Reca_l} \right) \quad (21)$$

The negative predictive value (NPV) is the proportion of negatively classified cases that were truly negative.

$$NPV = \frac{TN}{TN + FN} \quad (22)$$

The confusion matrices of the FCMM-RPS model on the weather prediction process under training (TR) and testing (TS) data are illustrated in Figure 3. The results reported that the FCMM-RPS model has properly identified the positive and negative classes of rainfall prediction in all cases.

Table 2 reports the overall rainfall prediction results of the FCMM-RPS model on 70% of TR and 30% of TS databases. Figure 4 offers a brief rainfall prediction performance of the FCMM-RPS model on 70% of the TR database. The figure highlights that the FCMM-RPS model has categorized all the samples under positive and negative classes. It is observed that the FCMM-RPS model has obtained an average $accu_{bal}$ of 94.75%, $prec_n$ of 93.13%, $reca_l$ of 94.75%, F_{score} of 93.92%, and NPV of 93.13%.

Table 2. Rainfall prediction outcomes of FCMM-RPS system on 70:30 of TR/TS databases.

Class	Accuracy _{bal}	Precision	Recall	F-Score	NPV
Training Phase (70%)					
Positive	98.77	99.15	98.77	98.96	87.12
Negative	90.73	87.12	90.73	88.89	99.15
Average	94.75	93.13	94.75	93.92	93.13
Testing Phase (30%)					
Positive	99.05	98.92	99.05	98.99	90.52
Negative	89.39	90.52	89.39	89.95	98.92
Average	94.22	94.72	94.22	94.47	94.72

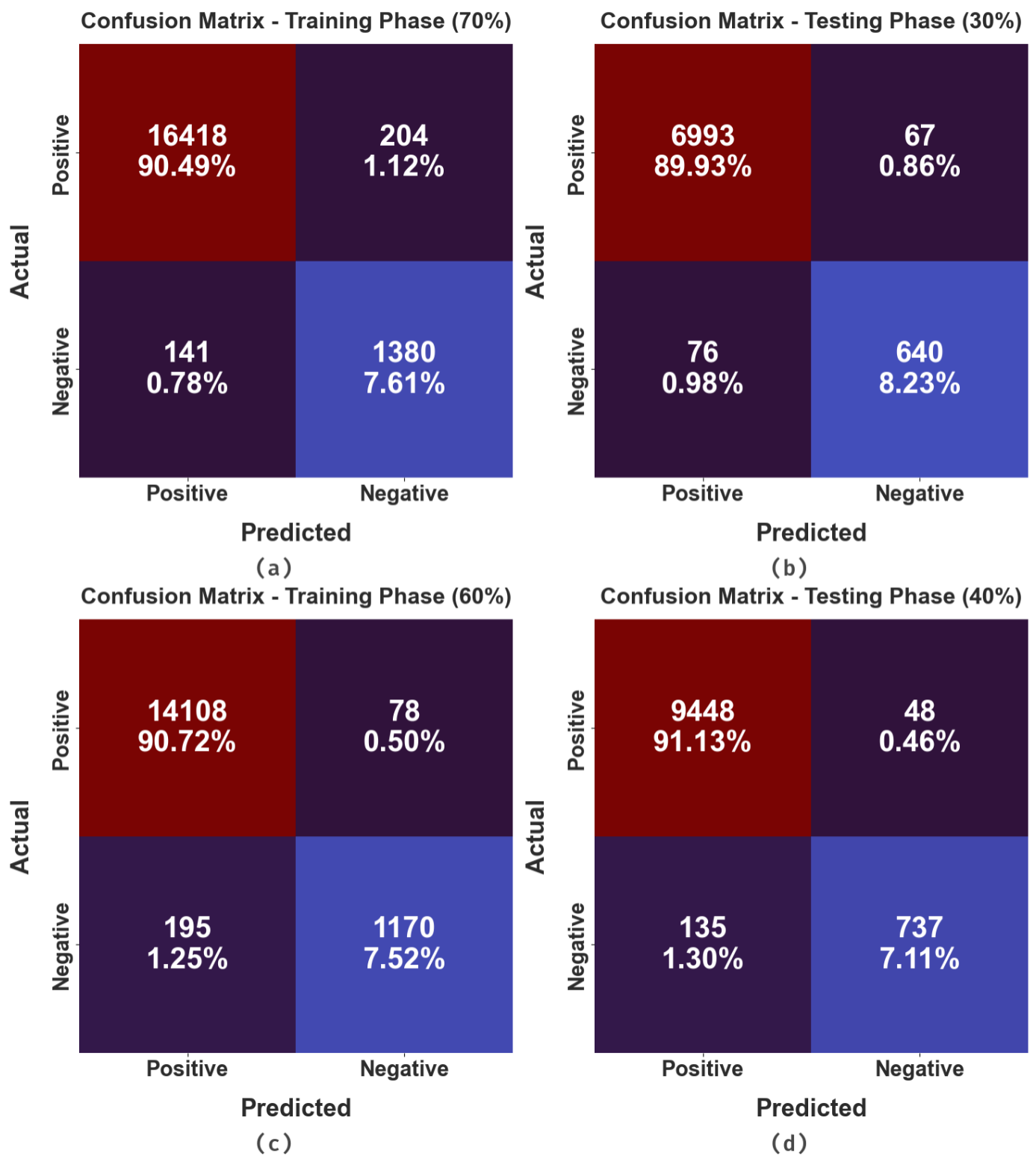


Figure 3. Confusion matrices of the FCMM-RPS system. (a,b) TR and TS databases of 70:30 and (c,d) TR and TS databases of 60:40.

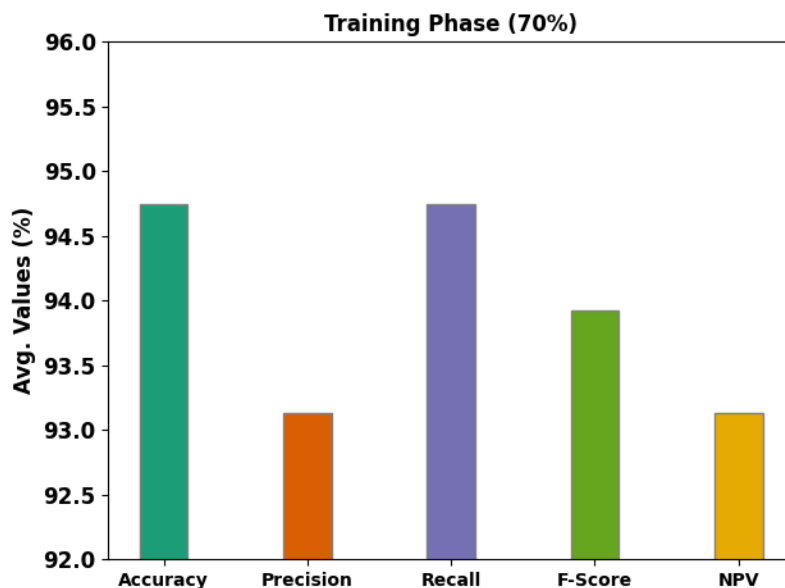


Figure 4. Average analysis of FCMM-RPS system on 80% of TR database.

Figure 5 provides the brief rainfall prediction performance of the FCMM-RPS method on 30% of the TS database. The figure emphasized that the FCMM-RPS approach has categorized all the samples under positive and negative classes. It is clear that the FCMM-RPS system has acquired an average $accu_{bal}$ of 94.22%, $prec_n$ of 94.72%, $reca_1$ of 94.22%, F_{score} of 94.47%, and NPV of 94.72%.

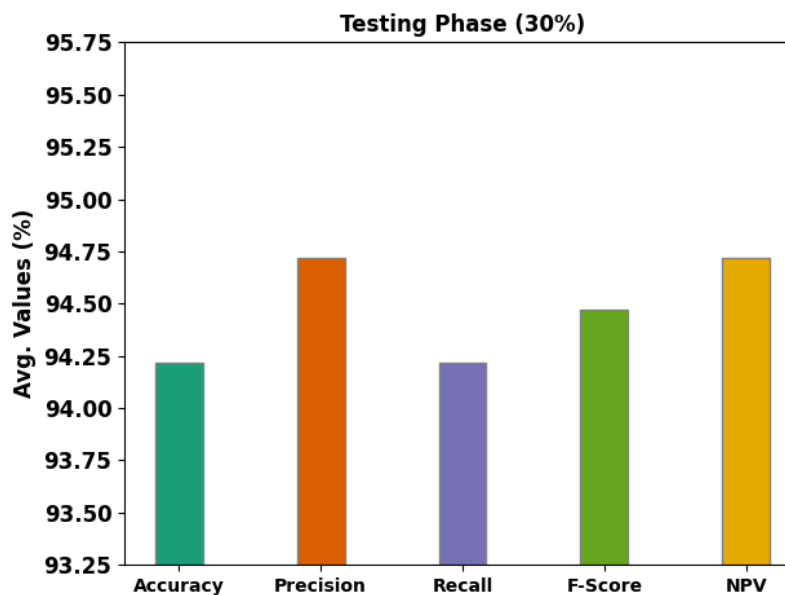


Figure 5. Average analysis of FCMM-RPS system on 70% of TR database.

Table 3 demonstrates the overall rainfall prediction outcomes of the FCMM-RPS algorithm on 60% of the TR database and 40% of the TS database. Figure 6 provides a brief rainfall prediction performance of the FCMM-RPS approach on 60% of the TR database. The figure shows that the FCMM-RPS method categorized all the samples into positive and negative classes. It is shown that the FCMM-RPS approach has attained an average $accu_{bal}$ of 92.58%, $prec_n$ of 96.19%, $reca_1$ of 92.58%, F_{score} of 94.30%, and NPV of 96.19%.

Table 3. Rainfall prediction outcome of FCMM-RPS system on 60:40 of TR/TS databases.

Class	Accuracy _{bal}	Precision	Recall	F-Score	NPV
Training Phase (60%)					
Positive	99.45	98.64	99.45	99.04	93.75
Negative	85.71	93.75	85.71	89.55	98.64
Average	92.58	96.19	92.58	94.30	96.19
Testing Phase (40%)					
Positive	99.49	98.59	99.49	99.04	93.89
Negative	84.52	93.89	84.52	88.96	98.59
Average	92.01	96.24	92.01	94.00	96.24

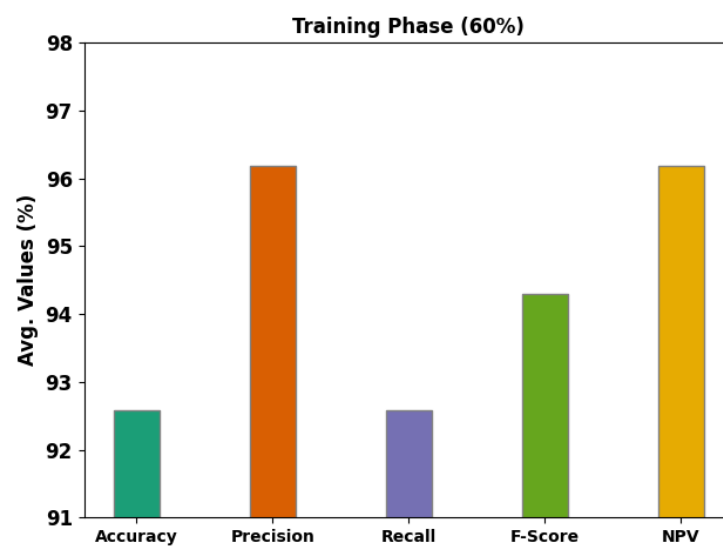
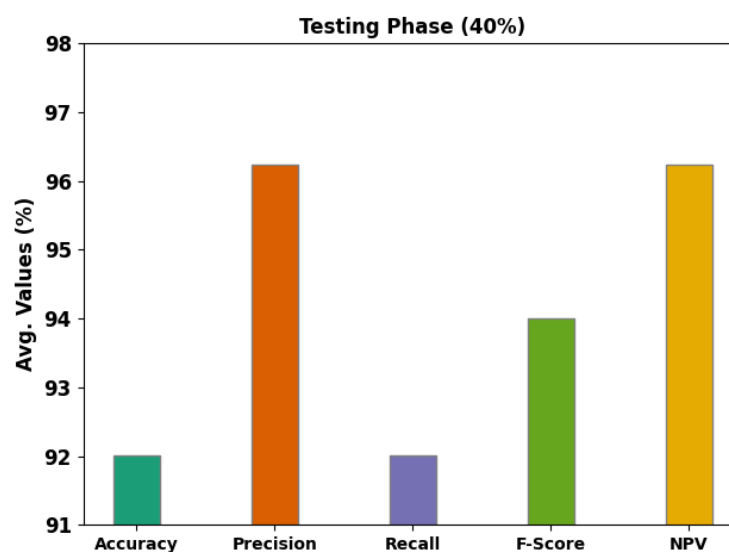
**Figure 6.** Average analysis of FCMM-RPS system on 60% of TR database.

Figure 7 depicts a brief rainfall prediction performance of the FCMM-RPS methodology on 40% of the TS database. The figure reveals that the FCMM-RPS method has categorized all the samples under positive and negative classes. It is detected that the FCMM-RPS system has gained an average $accu_{bal}$ of 92.01%, $prec_n$ of 96.24%, $reca_l$ of 92.01%, F_{score} of 94%, and NPV of 96.24%.

**Figure 7.** Average analysis of FCMM-RPS system on 40% of TS database.

The training accuracy (TACC) and validation accuracy (VACC) of the FCMM-RPS approach are examined on rainfall prediction performance in Figure 8. The figure shows that the FCMM-RPS methodology has exhibited enhanced performance with maximal values of TACC and VACC. It is observable that the FCMM-RPS approach has reached maximal TACC outcomes.



Figure 8. TACC and VACC analysis of FCMM-RPS system.

The training loss (TLS) and validation loss (VLS) of the FCMM-RPS methodology are tested on rainfall prediction performance in Figure 9. The figure shows that the FCMM-RPS algorithm has better performance with minimal values of TLS and VLS. It is noticeable that the FCMM-RPS system has resulted in lesser VLS outcomes.



Figure 9. TLS and VLS analysis of FCMM-RPS system.

An obvious precision–recall investigation of the FCMM-RPS approach on a test database is described in Figure 10. The figure reveals that the FCMM-RPS system has resulted in higher values of precision–recall values in various classes.

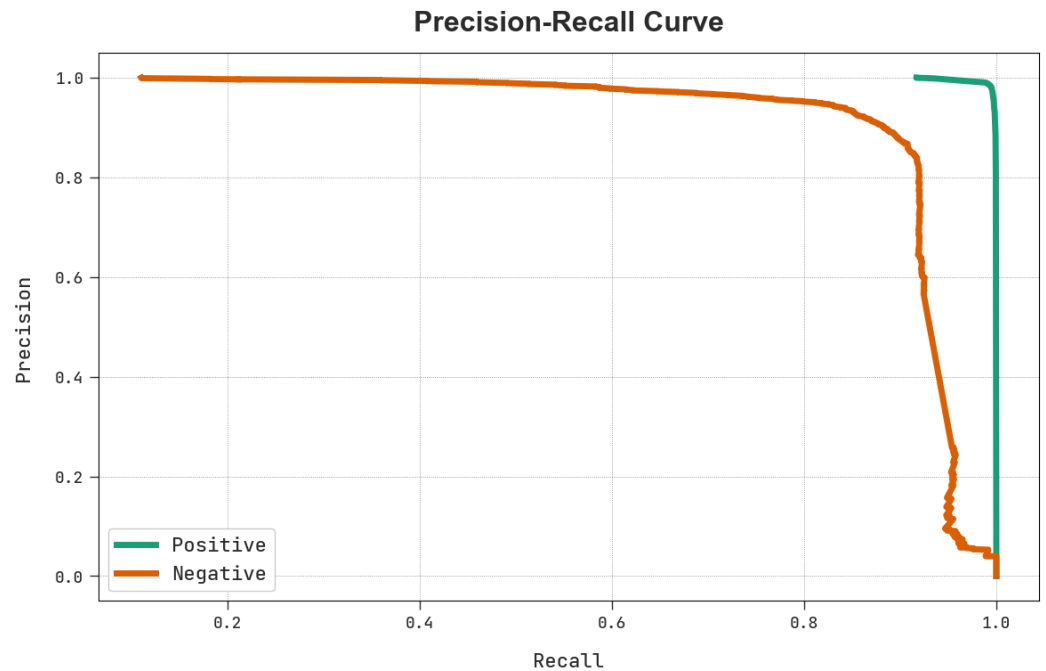


Figure 10. Precision–recall analysis of FCMM-RPS system.

Table 4 represent detailed results of the FCMM-RPS model with recent models [11]. The results show the enhanced outcomes of the FCMM-RPS model under all measures. Based on $accu_y$, the FCMM-RPS model has obtained a higher $accu_y$ of 94.22% while the FCM, decision tree (DT), Naïve Bayes (NB), K-nearest neighbor (KNN), support vector machine (SVM), and fused ML models have attained lower $accu_y$ values of 93.99%, 92.53%, 90.37%, 92.93%, 93.30%, and 93.94%, respectively. Meanwhile, with respect to $prec_n$, the FCMM-RPS algorithm has gained a superior $prec_n$ of 94.72% while the FCM, DT, NB, KNN, SVM, and fused ML approaches have reached minimal $prec_n$ values of 85.45%, 69.49%, 40.98%, 77.25%, 72.10%, and 84.03%, respectively. Furthermore, in terms of negative predictive value (NPV), the FCMM-RPS algorithm has obtained an enhanced NPV of 94.72% while the FCM, DT, NB, KNN, SVM, and fused ML systems have attained decreased NPVs of 94.54%, 93.62%, 93.62%, 93.47%, 93.07%, and 94.20%, respectively. These results assure the enhanced performance of the FCMM-RPS model. The enhanced performance of the proposed model is due to the parameter-tuning process by MBOA. In addition, the data preprocessing including missing value removal and data normalization process helps to improve the quality of the input rainfall data. Further, the advantages of the FCM model and MBOA include an improved rainfall prediction process over other existing models.

Table 4. Comparative analysis of FCMM-RPS system with existing approaches [11].

Methods	Accuracy	Precision	NPV
FCMM-RPS	94.22	94.72	94.72
FCM	93.99	85.45	94.54
Decision tree [23]	92.53	69.49	93.62
Naïve Bayes [23]	90.37	40.98	93.47
KNN [23]	92.93	77.25	91.37
SVM [11]	93.30	72.10	93.07
Fused ML [11]	93.94	84.03	94.20

5. Conclusions

In this article, we have introduced a new FCMM-RPS technique for predicting rainfall accurately. The major aim of the FCMM-RPS technique is to forecast rainfall routinely and efficiently. The presented FCMM-RPS technique primarily preprocessed the rainfall data to make it compatible. In addition, the presented FCMM-RPS technique predicts rainfall using the FCM model. To enhance the rainfall prediction outcomes of the FCM model, the parameter optimization process was performed using the MBOA. The performance assessment of the FCMM-RPS technique was tested on a rainfall dataset. A widespread comparison study highlighted the improvements of the FCMM-RPS technique in the rainfall forecasting process compared to existing techniques with a maximum accuracy of 94.22%. Thus, the presented FCMM-RPS technique can be employed for automated rainfall forecasting in real time. In the future, the prediction accuracy can be boosted by the use of sensor and meteorological datasets with additional different environmental features. Hence, in future work, big data analysis can be used for rainfall prediction if the sensor and meteorological datasets are used for the daily rainfall amount prediction study.

Author Contributions: Conceptualization, M.A.D. and I.Y.; Methodology, J.S.A. and M.I.A.; Software, A.S.Z. and I.Y.; Validation, H.G.M., J.S.A., M.M., I.Y. and M.I.A.; Formal analysis, R.A.; Investigation, A.S.Z.; Resources, M.M. and M.I.A.; Data curation, R.A. and M.M.; Writing—original draft, M.A.D., H.G.M., J.S.A. and R.A.; Writing—review & editing, A.S.Z., I.Y. and M.I.A.; Visualization, M.M.; Project administration, M.A.D.; Funding acquisition, H.G.M. All authors have read and agreed to the published version of the manuscript.

Funding: Princess Nourah bint Abdulrahman University Researchers Supporting Project number (PNURSP2022R140), Princess Nourah bint Abdulrahman University, Riyadh, Saudi Arabia. The authors would like to thank the Deanship of Scientific Research at Umm Al-Qura University for supporting this work by Grant Code: 22UQU4340237DSR60.

Institutional Review Board Statement: This article does not contain any studies with human participants performed by any of the authors. Not applicable.

Informed Consent Statement: Not applicable.

Data Availability Statement: Data sharing is not applicable to this article as no datasets were generated during the current study.

Conflicts of Interest: The authors declare that they have no conflict of interest. The manuscript was written through the contributions of all authors. All authors have given approval for the final version of the manuscript.

References

1. Reddy, P.C.S.; Yadala, S.; Goddummarri, S.N. Development of rainfall forecasting model using machine learning with singular spectrum analysis. *IIUM Eng. J.* **2022**, *23*, 172–186. [[CrossRef](#)]
2. Basha, C.Z.; Bhavana, N.; Bhavya, P.; Sowmya, V. Rainfall prediction using machine learning & deep learning techniques. In Proceedings of the 2020 International Conference on Electronics and Sustainable Communication Systems (ICESC), Coimbatore, India, 4–6 July 2020; pp. 92–97.
3. Fayaz, S.A.; Zaman, M.; Butt, M.A. Knowledge discovery in geographical sciences—A systematic survey of various machine learning algorithms for rainfall prediction. In *International Conference on Innovative Computing and Communications*; Khanna, A., Gupta, D., Bhattacharyya, S., Hassanien, A.E., Anand, S., Jaiswal, A., Eds.; Springer: Singapore, 2022; pp. 593–608.
4. Ridwan, W.M.; Sapitang, M.; Aziz, A.; Kushiari, K.F.; Ahmed, A.N.; El-Shafie, A. Rainfall forecasting model using machine learning methods: Case study Terengganu, Malaysia. *Ain Shams Eng. J.* **2021**, *12*, 1651–1663. [[CrossRef](#)]
5. Moon, S.H.; Kim, Y.H.; Lee, Y.H.; Moon, B.R. Application of machine learning to an early warning system for very short-term heavy rainfall. *J. Hydrol.* **2019**, *568*, 1042–1054. [[CrossRef](#)]
6. Diez-Sierra, J.; Del Jesus, M. Long-term rainfall prediction using atmospheric synoptic patterns in semi-arid climates with statistical and machine learning methods. *J. Hydrol.* **2020**, *586*, 124789. [[CrossRef](#)]
7. Hussein, E.A.; Ghaziasgar, M.; Thron, C.; Vaccari, M.; Jafta, Y. Rainfall Prediction Using Machine Learning Models: Literature Survey. In *Artificial Intelligence for Data Science in Theory and Practice*; Alloghani, M., Thron, C., Subair, S., Eds.; Springer: Berlin/Heidelberg, Germany, 2022; pp. 75–108.
8. Khan, M.I.; Maity, R. Hybrid deep learning approach for multi-step-ahead daily rainfall prediction using GCM simulations. *IEEE Access* **2020**, *8*, 52774–52784. [[CrossRef](#)]

9. Chao, Z.; Pu, F.; Yin, Y.; Han, B.; Chen, X. Research on real-time local rainfall prediction based on MEMS sensors. *J. Sens.* **2018**, *2018*, 6184713. [[CrossRef](#)]
10. Chhetri, M.; Kumar, S.; Pratim Roy, P.; Kim, B.G. Deep BLSTM-GRU model for monthly rainfall prediction: A case study of Simtokha, Bhutan. *Remote Sens.* **2020**, *12*, 3174. [[CrossRef](#)]
11. Rahman, A.U.; Abbas, S.; Gollapalli, M.; Ahmed, R.; Aftab, S.; Ahmad, M.; Khan, M.A.; Mosavi, A. Rainfall Prediction System Using Machine Learning Fusion for Smart Cities. *Sensors* **2022**, *22*, 3504. [[CrossRef](#)] [[PubMed](#)]
12. Pathan, M.S.; Nag, A.; Dev, S. Efficient rainfall prediction using a dimensionality reduction method. In Proceedings of the IGARSS 2022—2022 IEEE International Geoscience and Remote Sensing Symposium, Kuala Lumpur, Malaysia, 17–22 July 2022; pp. 6737–6740.
13. Poornima, S.; Pushpalatha, M. Prediction of rainfall using intensified LSTM based recurrent neural network with weighted linear units. *Atmosphere* **2019**, *10*, 668. [[CrossRef](#)]
14. He, R.; Zhang, L.; Chew, A.W.Z. Modeling and predicting rainfall time series using seasonal-trend decomposition and machine learning. *Knowl. Based Syst.* **2022**, *251*, 109125. [[CrossRef](#)]
15. Kala, A.; Vaidyanathan, S.G. Prediction of rainfall using artificial neural network. In Proceedings of the 2018 International Conference on Inventive Research in Computing Applications (ICIRCA), Coimbatore, India, 11–12 July 2018; pp. 339–342.
16. Wei, C.C.; Chou, T.H. Typhoon quantitative rainfall prediction from big data analytics by using the apache hadoop spark parallel computing framework. *Atmosphere* **2020**, *11*, 870. [[CrossRef](#)]
17. Samad, A.; Gautam, V.; Jain, P.; Sarkar, K. An approach for rainfall prediction using long short term memory neural network. In Proceedings of the 2020 IEEE 5th International Conference on Computing Communication and Automation (ICCCA), Greater Noida, India, 30–31 October 2020; pp. 190–195.
18. Kosko, B. Fuzzy cognitive maps. *Int. J. Man Mach. Stud.* **1986**, *24*, 65–75. [[CrossRef](#)]
19. Kociołek, M.; Strzelecki, M.; Obuchowicz, R. Does image normalization and intensity resolution impact texture classification? *Comput. Med. Imaging Graph.* **2020**, *81*, 101716. [[CrossRef](#)] [[PubMed](#)]
20. Behrooz, F.; Mariun, N.; Marhaban, M.H.; Mohd Radzi, M.A.; Ramli, A.R. Review of control techniques for HVAC systems—Nonlinearity approaches based on Fuzzy cognitive maps. *Energies* **2018**, *11*, 495. [[CrossRef](#)]
21. Long, W.; Wu, T.; Xu, M.; Tang, M.; Cai, S. Parameters identification of photovoltaic models by using an enhanced adaptive butterfly optimization algorithm. *Energy* **2021**, *229*, 120750. [[CrossRef](#)]
22. Dong, X.; Chu, T.; Huang, T.; Ji, Z.; Wu, S. Noisy Adaptation Generates Lévy Flights in Attractor Neural Networks. *Adv. Neural Inf. Process. Syst.* **2021**, *34*, 16791–16804.
23. Gupta, D.; Ghose, U. A comparative study of classification algorithms for forecasting rainfall. In Proceedings of the 2015 4th International Conference on Reliability, Infocom Technologies and Optimization (ICRITO) Trends and Future Directions, Noida, India, 2–4 September 2015; pp. 1–6.

Disclaimer/Publisher’s Note: The statements, opinions and data contained in all publications are solely those of the individual author(s) and contributor(s) and not of MDPI and/or the editor(s). MDPI and/or the editor(s) disclaim responsibility for any injury to people or property resulting from any ideas, methods, instructions or products referred to in the content.